

# Ongoing Astrometric Microlensing Events of Two Nearby Stars

J. Klüter, U. Bastian, M. Demleitner, J. Wambsganss

Zentrum für Astronomie der Universität Heidelberg, Astronomisches Rechen-Institut, Mönchhofstr. 12, 69120 Heidelberg, Germany  
e-mail: klueter@ari.uni-heidelberg.de

Received May ?, 2018; accepted ???, ???

## ABSTRACT

**Context.** Astrometric microlensing is an excellent tool to determine the mass of a stellar object. By measuring the astrometric shift of a background source star in combination with precise predictions of its unlensed position and of the lens position, gravitational lensing allows to determine the mass of the lensing star with a precision of 1 percent, independent of any prior knowledge.

**Aims.** Making use of the recently published Gaia Data Release 2 (*Gaia* DR2) we predict astrometric microlensing events by foreground stars of high proper motion passing by a background star in the coming years.

**Methods.** We compile a list of  $\sim 148.000$  high-proper-motion stars within *Gaia* DR2 with  $\mu_{tot} > 150$  mas/yr. We then search for background stars close to their paths and calculate the dates and separations of the closest approaches. Using color and absolute magnitude, we determine approximate masses of the lenses. Finally, we calculate the expected astrometric shifts and magnifications of the predicted events.

**Results.** We detect two ongoing microlensing events by the high proper motion stars Luyten 143-23 and Ross 322 and predict closest separations of  $(108.5 \pm 1.4)$  mas in July 2018 and  $(125.3 \pm 3.4)$  mas in August 2018, respectively. The respective expected astrometric shifts are  $(1.74 \pm 0.12)$  mas and  $(0.76 \pm 0.06)$  mas. Furthermore, Luyten 143-23 will pass by another star in March 2021 with a closest separation of  $(280.1 \pm 1.1)$  mas, which results in an expected shift of  $(0.69 \pm 0.05)$  mas.

**Key words.** astrometry – Proper motions – Catalogs – Gravitational lensing: micro

## 1. Introduction

Gravitational lensing is a powerful tool to probe our universe on very different mass and distance scales, from exoplanets in the Milky Way to multiply imaged quasars and giant arcs at cosmological distance scales. When a foreground star (“lens”) passes a background star (“source”), two effects can be observed due to gravitational lensing: A magnification of the source (photometric microlensing), and a shift of the source position (astrometric microlensing). Whereas more than 10,000 photometric microlensing events have been observed – including a few dozen extrasolar planet detections (e.g., Udalski et al. 2015), astrometric microlensing was detected for the first time only recently (Kains et al. 2017). Due to its dependence on mass, astrometric microlensing is one of the few possibilities to “weigh” stellar objects with a precision of about one percent (Paczynski 1995).

For photometric microlensing, the impact parameter between lens and source needs to be of order the angular Einstein radius or smaller ( $\Delta\theta \lesssim 1\theta_E$ ) for measurable effects. Astrometric microlensing can be detected at much larger angular separations between lens and source (i.e.,  $\Delta\theta \gg 1\theta_E$ ). Furthermore, it is possible to *predict* astrometric microlensing events from precise proper motions and positions of lens and source (Paczynski 1995). For the prediction of astrometric events, in particular faint nearby stars with high proper motions are of interest. High proper motions are preferred, because the covered area within a given time is larger, hence microlensing events are more likely. Furthermore, a high proper motion leads to a significant positional shift on a shorter time scale. Nearby stars are preferred, because their Einstein radius is larger and therefore the expected shift is also larger. And faint lenses are favourable, since the measurement of the source position is less contaminated by the

lens. Astrometric microlensing events were already predicted by, e.g., Proft et al. (2011); Sahu et al. (2014); McGill et al. (2018). The second data release of *Gaia* (*Gaia* DR2, Gaia Collaboration et al. 2018) now provides a highly improved data set for such studies. Not only the proper motions of the lenses are provided by *Gaia* DR2, but also precise parallaxes which are needed to calculate the mass of the lens afterwards, as well as the proper motion of the source. These big improvements in data quality and quantity lead to much more precise predictions. In addition, the excellent resolution and accuracy of *Gaia* provides the opportunity to actually measure the predicted shifts of the background sources. Hence the events during the *Gaia* Mission are of particularly high scientific interest.

This letter is structured as follows: In Section 2 we explain the basics of our method, in Section 3 we present the predicted microlensing events of two nearby stars. We summarize our results and present conclusions in Section 4.

## 2. Method

We use a method similar to that of Proft et al. (2011) in order to search for new astrometric microlensing events. Here we briefly delineate the main steps of our method; the complete method will be detailed in an upcoming paper (Klüter et al. in prep.).

We start with a list of high-proper-motion stars ( $\mu_{tot} > 150$  mas/yr) from *Gaia* DR2 and use the following quality cuts to eliminate possibly erroneous data:  $\varpi > 8\sigma_\varpi$ ,  $\varpi/\mu_{tot} < 0.5$  yr and  $phot\_g\_n\_obs^2 \cdot phot\_g\_flux\_over\_error > 10^6$

About  $\sim 148.000$  stars fulfill these criteria. For those potential lenses we search for background stars in a rectangular box defined by the J2015.5 positions and the positions in 50 years,

arXiv:1805.08023v1 [astro-ph.SR] 21 May 2018

with a box width of  $\pm 7''$  perpendicular to the direction of the proper motion. In the following, the combination of a high-proper-motion foreground lens and a background source is called “candidate”. The source parameters are labeled with the prefix “Sou\_”. To avoid binary stars in our candidate list, we exclude common proper motion pairs. Using the *Gaia* DR2 positions, proper motions and parallaxes, we then determine the minimum separation between source and lens, and the epoch of closest approach.

In order to get a realistic value for the expected astrometric shifts of our candidates, we estimate an approximate mass for the lens in the following way. We sort the potential lenses into the three classes white dwarfs (WD), main sequence stars and red giants (RG), by using the following cuts:

$$WD : G_{BP,abs} \geq 4 \cdot (G - G_{RP})^2 + 4.5 \cdot (G - G_{RP}) + 6 \quad (1)$$

$$RG : G_{BP,abs} \leq -3 \cdot (G - G_{RP})^2 + 8 \cdot (G - G_{RP}) - 1.3$$

For white dwarfs and red giants we use approximate masses of  $(0.65 \pm 0.15) M_{\odot}$  and  $(1.0 \pm 0.5) M_{\odot}$ , respectively. For main-sequence stars we use the following relation with *G* magnitude, determined from a list of temperatures and stellar radii for different stellar types (Pecaut & Mamajek 2013), the translation between *Gaia* and Johnson filters (Jordi et al. 2010), and mass-luminosity relations (Salaris & Cassisi 2005):

$$(G_{abs} < 8.85) :$$

$$\log\left(\frac{M}{M_{\odot}}\right) = 0.00786 G_{abs}^2 - 0.290 G_{abs} + 1.18$$

$$(8.85 < G_{abs} < 15) :$$

$$\log\left(\frac{M}{M_{\odot}}\right) = -0.301 G_{abs} + 1.89$$

$$(15 < G_{abs}) :$$

$$M = 0.07 M_{\odot}$$

The first two relations are due to different slopes in the mass-luminosity relations, the third one is for brown dwarfs. For main-sequence stars we consider an error of 10%. We also use these equations when *Gaia* DR2 does not provide color information for the lens, i.e., we assume those stars are main-sequence stars. As the next step, we calculate the angular Einstein radii from the masses and the *Gaia* DR2 parallaxes:

$$\theta_E = 2.854 \text{ mas} \sqrt{\frac{M}{M_{\odot}} \cdot \frac{\varpi - \text{Sou}_{\varpi}}{1 \text{ mas}}} \quad (3)$$

Finally, we determine the expected shift of the center of light (Paczynski 1998)

$$\delta\theta_c = \frac{u}{u^2 + 2} \cdot \theta_E, \quad (4)$$

where  $u$  is the angular separation in units of  $\theta_E$ . We note that Eq. 4 is only valid when source and lens can be resolved, otherwise luminous-lens effects have to be considered.

### 3. Astrometric Microlensing Event

We found and report here two currently ongoing astrometric microlensing events by the high proper motion stars Luyten 143-23 and Ross 322. The expected maximum shifts are  $(1.74 \pm 0.12) \text{ mas}$  and  $(0.76 \pm 0.06) \text{ mas}$ , respectively.

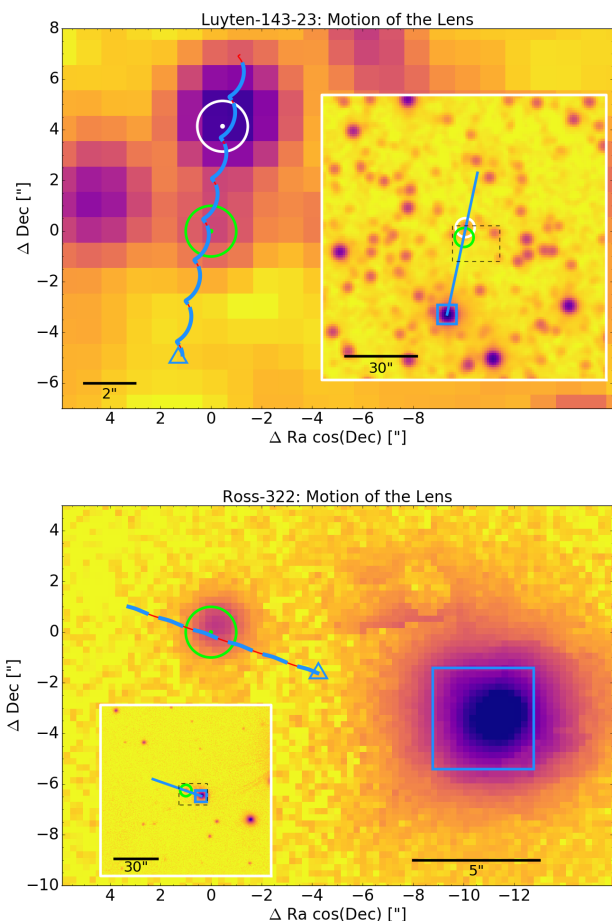


**Fig. 1.** The top panel shows a 2MASS image with the two background stars that Luyten 143-23 passes by in July 2018 (green circle) and in March 2021 (white circle), respectively. The bottom panel shows a Pan-STARRS image with the background star which Ross 322 passes by in August 2018 (green circle). The exact positions of the background sources are indicated with small dots at the centers of the circles. Their motions and the uncertainties are smaller than the size of the dots. The triangles indicate the J2015.5 positions of the lens stars measured by *Gaia*. The predicted motions are shown as thick blue/thin red curves, where the thin red parts indicate the epochs at which the stars cannot be observed. In both panels, the original positions (at earlier epochs) of the lens stars in the 2MASS and PanSTARRS images are indicated as squares. Larger views of the sky areas are displayed in the insets. The blue lines in the insets show the motion of the lens stars until 2035.

#### 3.1. Luyten 143-23

Luyten 143-23 is an M dwarf (M4V) with a parallax of 206.8 mas and an absolute proper motion of 1647.2 mas/yr. Its apparent *G* magnitude is 11.9 mag (see Tab. 1 for more details). By using our  $G_{abs} - \text{Mass}$  relation (Eq. 2) we determine an approximate mass of  $0.12 M_{\odot}$ . We found that it currently passes a  $G = 18.5 \text{ mag}$  star with a closest approach on July 7, 2018 and a smallest separation of 108.53 mas. Position, proper motion, parallax and magnitudes for the background source star are given in the top part of Tab. 2, information on the closest approach can be found in the bottom part of Tab. 2. The top panel of Fig. 1 shows a 2MASS (Skrutskie et al. 2006) image of Luyten 143-23, the interesting background star is marked with a green circle. The motion of the background star within 5 years and the positional uncertainties are smaller than the centered dot. The predicted path of Luyten 143-23 is shown as a thick blue/thin red line,

**Table 1.** Important *Gaia* DR2 parameters for the lenses. Listed are source ID (*ID*), J2015.5 position (*Ra*, *Dec*), proper motion ( $\mu$ ), parallax( $\varpi$ ), and magnitude (*G*, *G<sub>RP</sub>*, *G<sub>BP</sub>*) for the lens stars. Further information for the lens stars can be extracted from *Gaia* DR2 using the Source Id.

	Luyten 143-23	Ross 322
<i>ID</i>	5254061535097566848	314922605759778048
<i>Ra</i>	161.085375416°	16.956492031°
<i>Dec</i>	-61.202862014°	34.210553416°
$\sigma_{Ra}$	0.10 mas	0.05 mas
$\sigma_{Dec}$	0.13 mas	0.04 mas
$\mu_{Ra}$	-346.43 mas/yr	1373.67 mas/yr
$\mu_{Dec}$	1610.34 mas/yr	-480.33 mas/yr
$\sigma_{\mu_{Ra}}$	0.17 mas/yr	0.09 mas/yr
$\sigma_{\mu_{Dec}}$	0.25 mas/yr	0.08 mas/yr
$\varpi$	206.82 mas	42.51 mas
$\sigma_{\varpi}$	0.08 mas	0.05 mas
<i>G</i>	11.9 mag	12.4 mag
<i>G<sub>RP</sub></i>	10.9 mag	11.3 mag
<i>G<sub>BP</sub></i>	14.2 mag	13.6 mag

where the red parts indicate the times at which Luyten 143-23 is not observable. The blue triangle indicates its J2015.5 position listed by *Gaia* DR2. We note that the observability is only a rough estimate, since it depends on the location of the observatory and the capability of the instruments.

Due to the large Einstein radius of  $\theta_E = 14.0$  mas, caused by the small distance of Luyten 143-23, a maximum shift of  $(1.74 \pm 0.12)$  mas is expected. The unlensed motion of the background star as well as the predicted path due to lensing are shown in the top panel of Fig. 2. Finally, the absolute shift as a function of time is displayed in the top panel of Fig. 3. Due to the high proper motion of Luyten 143-23 we expect a rapid change of the astrometric shift between June and September 2018 ( $1.3$  mas in 3 months). Unfortunately, Luyten 143-23 is not observable in August/September 2018 from the ground or by *Gaia*.

We found a further close encounter of Luyten 143-23 with a  $G = 17.0$  mag star to occur in 2021. The smallest separation of  $(280.1 \pm 1.1)$  mas is reached at March 9, 2021, we expect a maximum shift of  $(0.69 \pm 0.05)$  mas. This background star is marked with a white circle in Fig. 1. The expected motion and the astrometric shift are shown in the middle panels of Figs. 2 + 3.

### 3.2. Ross 322

Ross 322 is an M dwarf (M2V) with a parallax of 42.5 mas. Its absolute proper motion is 1455.2 mas/yr (Tab. 1). We determine an approximate mass of  $0.28 M_{\odot}$ . Ross 322 currently passes by a  $G = 18.6$  mag star with a closest approach at August 8, 2018, with a separation of  $(125.3 \pm 3.4)$  mas. Since the Einstein radius of Ross 322 is smaller than that of Luyten 143-23 the expected shift is only  $(0.76 \pm 0.06)$  mas. However, this should still be measurable with sufficient accuracy. The important parameters are also displayed in Tab. 2 and the same plots as for Luyten 143-23 are given in the bottom panels of Fig. 1 - 3, superposed on a Pan-STARRS image (Chambers & Pan-STARRS Team 2018).

## 4. Summary and Conclusions

We report two ongoing astrometric microlensing events by the two nearby stars Luyten 143-23 and Ross 322. They reach their closest approaches in July 2018 and August 2018, respectively.

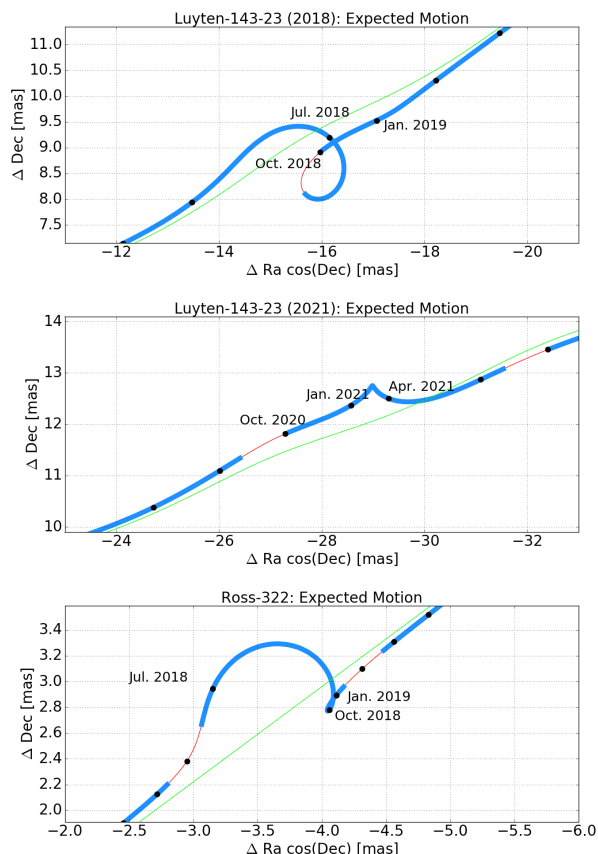


**Fig. 2.** Predicted motions of the background stars for the events by Luyten 143-23 in 2018 (Top), in 2021 (Middle), and by Ross 322 in 2018 (Bottom). The origin of the coordinate system is the background star's J2015.5 position. The thin green lines show the unaffected motions of the background stars, the expected paths are shown as thick blue/thin red lines (red parts indicate the epochs at which the star is not observable). The black dots indicate equal time intervals of 3 months.

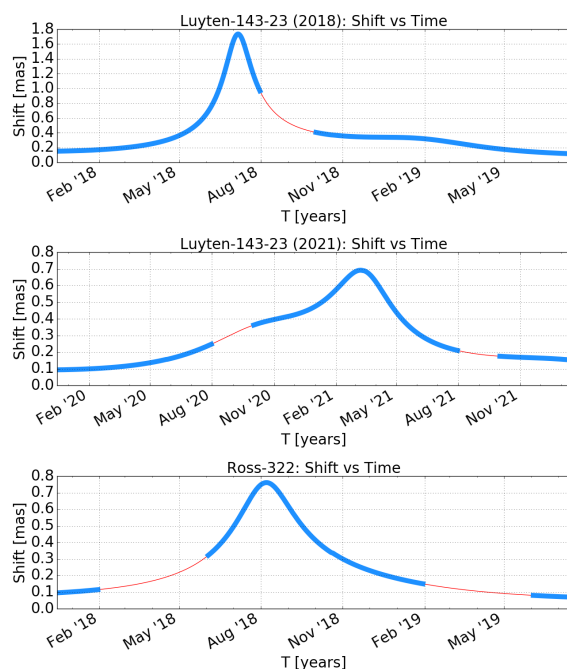


**Fig. 3.** Expected shifts as function of time for events by Luyten 143-23 in 2018 (Top), in 2021 (Middle), and by Ross 322 in 2018 (Bottom). The thin red parts indicate the epochs at which the star is not observable.

**Table 2.** Important parameters for the astrometric microlensing events reported here. The table lists source ID (*Sou\_ID*), J2015.5 position (*Sou\_Ra*, *Sou\_Dec*), proper motion (*Sou\_μ*) parallax(*Sou\_ϖ*), and G magnitude (*Sou\_G*, *Sou\_G<sub>RP</sub>*, *Sou\_G<sub>BP</sub>*) for the background stars, furthermore the angular Einstein radii ( $\theta_E$ ), epoch and distance of closest approach ( $T_{min}$ ,  $D_{min}$ ), and the maximum expected shifts ( $\Delta\theta_{max}$ ). Further information for the background stars can be extracted from *Gaia* DR2 using the Source ID.

	Luyten 143-23 (2018)	Luyten 143-23 (2021)	Ross 322 (2018)
<i>Sou_ID</i>	5254061535052907008	5254061535097574016	314922601464808064
<i>Sou_Ra</i>	161.08462829°	161.08436459°	16.95791867°
<i>Sou_Dec</i>	-61.20147495°	-61.20032468°	+34.21100433°
<i>Sou_σ<sub>Ra</sub></i>	0.16 mas	0.06 mas	0.27 mas
<i>Sou_σ<sub>Dec</sub></i>	0.16 mas	0.06 mas	0.38 mas
<i>Sou_μ<sub>Ra</sub></i>	-4.85 mas/yr	-5.20 mas/yr	-1.12 mas/yr
<i>Sou_μ<sub>Dec</sub></i>	2.82 mas/yr	2.17 mas/yr	0.83 mas/yr
<i>Sou_σ<sub>μ<sub>Ra</sub></sub></i>	0.38 mas/yr	0.13 mas/yr	0.60 mas/yr
<i>Sou_σ<sub>μ<sub>Dec</sub></sub></i>	0.33 mas/yr	0.12 mas/yr	0.62 mas/yr
<i>Sou_ϖ</i>	0.09 mas	0.07 mas	-0.05 mas
<i>Sou_σ<sub>ϖ</sub></i>	0.19 mas	0.07 mas	0.44 mas
<i>Sou_G</i>	18.5 mag	17.0 mag	18.6 mag
<i>Sou_G<sub>RP</sub></i>	16.9 mag	15.9 mag	17.6 mag
<i>Sou_G<sub>BP</sub></i>	19.1 mag	18.0 mag	18.6 mag
$\theta_E$	14.0 mas	14.0 mas	9.8 mas
$\sigma\theta_E$	0.7 mas	0.7 mas	0.5 mas
$T_{min}$ (TCB)	J2018.51236 yr	J2021.18674 yr	J2018.5995 yr
$\sigma T_{min}$	0.00051 yr	0.00063 yr	0.0022 yr
$D_{min}$	108.5 mas	280.1 mas	125.3 mas
$\sigma D_{min}$	1.4 mas	1.1 mas	3.4 mas
$\Delta\theta_{max}$	1.74 mas	0.69 mas	0.76 mas
$\sigma\Delta\theta_{max}$	0.12 mas	0.05 mas	0.06 mas

Due to the precise data of *Gaia* DR2, we were able to predict the separations between foreground and background stars as a function of time with an accuracy of a few percent and the time of the closest approach with an accuracy of a few hours. Because of the large Einstein radii (14.0 mas; 9.8 mas), we expect a measurable effect even though the minimum separation is above 100 mas. Luyten 143-23 will pass a further star in March 2021 with a closest separation of 280.1 mas and an expected shift of 0.69 mas. For these separations it is also possible to resolve both stars with high resolution instruments such as GRAVITY (Gravity Collaboration et al. 2017), although the background source is  $\sim 5$  magnitudes fainter (K band) than the lens. Further, the high proper motions of the lenses lead to a fast change of the astrometric shifts. Hence, both events are ideal to monitor with high-accurate astrometric instruments like *Gaia*, GRAVITY, Keck, or LBT. Due to the precise prediction, observations of both events offer the possibility to determine the masses of the two nearby high proper motion stars Luyten 143-23 and Ross 322 with a precision of a few percent. An initiative to acquire observations with GRAVITY and at the Keck Telescope during the two ongoing events has been launched by the authors.

*Acknowledgements.* This work has made use of results from the ESA space mission *Gaia*, the data from which were processed by the *Gaia* Data Processing and Analysis Consortium (DPAC). Funding for the DPAC has been provided by national institutions, in particular the institutions participating in the *Gaia* Multilateral Agreement. The *Gaia* mission website is: <http://www.cosmos.esa.int/Gaia>. Some of the authors are members of the *Gaia* Data Processing and Analysis Consortium (DPAC).

This publication makes use of data products from the Two Micron All Sky Survey, which is a joint project of the University of Massachusetts and the Infrared Processing and Analysis Center/California Institute of Technology, funded by the National Aeronautics and Space Administration and the National Science Foundation.

The Pan-STARRS1 Surveys (PS1) and the PS1 public science archive have been made possible through contributions by the Institute for Astronomy, the University of Hawaii, the Pan-STARRS Project Office, the Max-Planck Society and its

participating institutes, the Max Planck Institute for Astronomy, Heidelberg and the Max Planck Institute for Extraterrestrial Physics, Garching, The Johns Hopkins University, Durham University, the University of Edinburgh, the Queen's University Belfast, the Harvard-Smithsonian Center for Astrophysics, the Las Cumbres Souderservatory Global Telescope Network Incorporated, the National Central University of Taiwan, the Space Telescope Science Institute, the National Aeronautics and Space Administration under Grant No. NNX08AR22G issued through the Planetary Science Division of the NASA Science Mission Directorate, the National Science Foundation Grant No. AST-1238877, the University of Maryland, Eotvos Lorand University (ELTE), the Los Alamos National Laboratory, and the Gordon and Betty Moore Foundation.

This research has made use of the SIMBAD database, operated at CDS, Strasbourg, France.

We gratefully acknowledge the technical support we received from staff of the e-inf-astro project (BMBF Förderkennzeichen 05A17VH2).

## References

- Chambers, K. & Pan-STARRS Team. 2018, in American Astronomical Society Meeting Abstracts 231, 102.01
- Gaia Collaboration, Brown, A. G. A., Vallenari, A., et al. 2018, ArXiv e-prints [arXiv:1804.09365]
- Gravity Collaboration, Abuter, R., Accardo, M., et al. 2017, A&A, 602, A94
- Jordi, C., Gebran, M., Carrasco, J. M., et al. 2010, A&A, 523, A48
- Kains, N., Calamida, A., Sahu, K. C., et al. 2017, ApJ, 843, 145
- McGill, P., Smith, L. C., Wyn Evans, N., Belokurov, V., & Smart, R. L. 2018, MNRAS[arXiv:1804.07049]
- Paczynski, B. 1995, Acta Astron., 45, 345
- Paczynski, B. 1998, ApJ, 494, L23
- Pecaut, M. J. & Mamajek, E. E. 2013, ApJS, 208, 9
- Proft, S., Demleitner, M., & Wambsganss, J. 2011, A&A, 536, A50
- Sahu, K. C., Bond, H. E., Anderson, J., & Dominik, M. 2014, ApJ, 782, 89
- Salaris, M. & Cassisi, S. 2005, Evolution of Stars and Stellar Populations, 400
- Skrutskie, M. F., Cutri, R. M., Stiening, R., et al. 2006, AJ, 131, 1163
- Taylor, M. B. 2005, in Astronomical Society of the Pacific Conference Series, Vol. 347, Astronomical Data Analysis Software and Systems XIV, ed. P. Shopbell, M. Britton, & R. Ebert, 29
- Udalski, A., Szymański, M. K., & Szymański, G. 2015, Acta Astron., 65, 1